

<sup>1</sup> **Critical transitions and the fragmenting of global forests**

<sup>2</sup> **Leonardo A. Saravia<sup>1 3</sup>, Santiago R. Doyle<sup>1</sup>, Benjamin Bond-Lamberty<sup>2</sup>**

<sup>3</sup> 1. Instituto de Ciencias, Universidad Nacional de General Sarmiento, J.M. Gutierrez 1159 (1613), Los  
<sup>4</sup> Polvorines, Buenos Aires, Argentina.

<sup>5</sup> 2. Pacific Northwest National Laboratory, Joint Global Change Research Institute at the University of  
<sup>6</sup> Maryland–College Park, 5825 University Research Court #3500, College Park, MD 20740, USA

<sup>7</sup> 3. Corresponding author e-mail: lsaravia@ungs.edu.ar

<sup>8</sup> **keywords:** Forest fragmentation, early warning signals, percolation, power-laws, MODIS, critical transitions

<sup>9</sup> **Running title:** Critical fragmentation in global forest

<sup>10</sup> **Abstract**

<sup>11</sup> 1. Forests provide critical habitat for many species, essential ecosystem services, and are coupled to  
<sup>12</sup> atmospheric dynamics through exchanges of energy, water and gases. One of the most important  
<sup>13</sup> changes produced in the biosphere is the replacement of forest areas with human dominated landscapes.  
<sup>14</sup> This usually leads to fragmentation, altering the sizes of patches, the structure and function of the  
<sup>15</sup> forest. Here we studied the distribution and dynamics of forest patch sizes at a global level, examining  
<sup>16</sup> signals of a critical transition from an unfragmented to a fragmented state.

<sup>17</sup> 2. We used MODIS vegetation continuous field to estimate the forest patches at a global level and de-  
<sup>18</sup> fined wide regions of connected forest across continents and big islands. We search for critical phase  
<sup>19</sup> transitions, where the system state of the forest changes suddenly at a critical point in time; this  
<sup>20</sup> implies an abrupt change in connectivity that causes an increased fragmentation level. We studied the  
<sup>21</sup> distribution of forest patch sizes and the dynamics of the largest patch over the last fourteen years,  
<sup>22</sup> as the conditions that indicate that a region is near a critical fragmentation threshold are related to  
<sup>23</sup> patch size distribution and temporal fluctuations of the largest patch.

<sup>24</sup> 3. We found some evidence that allows us to analyze fragmentation as a critical transition: most regions  
<sup>25</sup> followed a power-law distribution over the 14 years. We also found that the Philippines region probably  
<sup>26</sup> went through a critical transition from a fragmented to an unfragmented state. Only the tropical forest  
<sup>27</sup> of Africa and South America met the criteria to be near a critical fragmentation threshold.

28     4. This implies that human pressures and climate forcings might trigger undesired effects of fragmentation,  
29       such as species loss and degradation of ecosystems services, in these regions. The simple criteria  
30       proposed here could be used as an early warning to estimate the distance to a fragmentation threshold  
31       in forest around the globe and a predictor of a planetary tipping point.

## **32    Introduction**

33    Forests are one of the most important biomes on earth, providing habitat for a large proportion of species  
34    and contributing extensively to global biodiversity (Crowther et al., 2015). In the previous century human  
35    activities have influenced global bio-geochemical cycles (Bonan, 2008; Canfield, Glazer, & Falkowski, 2010),  
36    with one of the most dramatic changes being the replacement of 40% of Earth's formerly biodiverse land  
37    areas with landscapes that contain only a few species of crop plants, domestic animals and humans (J. A.  
38    Foley et al., 2011). These local changes have accumulated over time and now constitute a global forcing  
39    (Barnosky et al., 2012).

40    Another global scale forcing that is tied to habitat destruction is fragmentation, which is defined as the  
41    division of a continuous habitat into separated portions that are smaller and more isolated. Fragmentation  
42    produces multiple interwoven effects: reductions of biodiversity between 13% and 75%, decreasing forest  
43    biomass, and changes in nutrient cycling (Haddad et al., 2015). The effects of fragmentation are not only  
44    important from an ecological point of view but also that of human activities, as ecosystem services are deeply  
45    influenced by the level of landscape fragmentation (Mitchell et al., 2015).

46    Ecosystems have complex interactions between species and present feedbacks at different levels of organiza-  
47    tion (Gilman, Urban, Tewksbury, Gilchrist, & Holt, 2010), and external forcings can produce abrupt changes  
48    from one state to another, called critical transitions (Scheffer et al., 2009). These abrupt state shifts cannot  
49    be linearly forecasted from past changes, and are thus difficult to predict and manage (Scheffer et al., 2009).  
50    Such 'critical' transitions have been detected mostly at local scales (S. R. Carpenter et al., 2011; Drake &  
51    Griffen, 2010), but the accumulation of changes in local communities that overlap geographically can prop-  
52    agate and theoretically cause an abrupt change of the entire system at larger scales (Barnosky et al., 2012).  
53    Coupled with the existence of global scale forcings, this implies the possibility that a critical transition could  
54    occur at a global scale (C. Folke et al., 2011; Rockstrom et al., 2009).

55    Complex systems can experience two general classes of critical transitions (R V Solé, 2011). In so-called first  
56    order transitions, a catastrophic regime shift that is mostly irreversible occurs because of the existence of  
57    alternative stable states (Scheffer et al., 2001). This class of transitions is suspected to be present in a variety  
58    of ecosystems such as lakes, woodlands, coral reefs (Scheffer et al., 2001), semi-arid grasslands (Brandon T.  
59    Bestelmeyer et al., 2011), and fish populations (Vasilakopoulos & Marshall, 2015). They can be the result of  
60    positive feedback mechanisms (Villa Martín, Bonachela, Levin, & Muñoz, 2015); for example, fires in some  
61    forest ecosystems were more likely to occur in previously burned areas than in unburned places (Kitzberger,  
62    Aráoz, Gowda, Mermoz, & Morales, 2012).

63 The other class of critical transitions are continuous or second order transitions (Ricard V. Solé & Bascompte,  
64 2006). In these cases, there is a narrow region where the system suddenly changes from one domain to another,  
65 with the change being continuous and in theory reversible. This kind of transitions were suggested to be  
66 present in tropical forest (S. Pueyo et al., 2010), semi-arid mountain ecosystems (McKenzie & Kennedy,  
67 2012), tundra shrublands (Naito & Cairns, 2015). The transition happens at a critical point where we can  
68 observe a distinctive spatial pattern: scale invariant fractal structures characterized by power law patch  
69 distributions (Stauffer & Aharony, 1994).

70 There are several processes that can convert a catastrophic transition to a second order transitions (Villa  
71 Martín et al., 2015). These include stochasticity, such as demographic fluctuations, spatial heterogeneities,  
72 and/or dispersal limitation. All these components are present in forest around the globe (Filotas et al.,  
73 2014; Fung, O'Dwyer, Rahman, Fletcher, & Chisholm, 2016; Seidler & Plotkin, 2006), and thus continuous  
74 transitions might be more probable than catastrophic transitions. Moreover there is some evidence of recovery  
75 in some systems that supposedly suffered an irreversible transition produced by overgrazing (Brandon T  
76 Bestelmeyer, Duniway, James, Burkett, & Havstad, 2013; J. Y. Zhang, Wang, Zhao, Xie, & Zhang, 2005)  
77 and desertification (Allington & Valone, 2010).

78 The spatial phenomena observed in continuous critical transitions deal with connectivity, a fundamental  
79 property of general systems and ecosystems from forests (Ochoa-Quintero, Gardner, Rosa, de Barros Ferraz,  
80 & Sutherland, 2015) to marine ecosystems (Leibold & Norberg, 2004) and the whole biosphere (Lenton &  
81 Williams, 2013). When a system goes from a fragmented to a connected state we say that it percolates (R  
82 V Solé, 2011). Percolation implies that there is a path of connections that involves the whole system. Thus  
83 we can characterize two domains or phases: one dominated by short-range interactions where information  
84 cannot spread, and another in which long range interactions are possible and information can spread over  
85 the whole area. (The term “information” is used in a broad sense and can represent species dispersal or  
86 movement.)

87 Thus, there is a critical “percolation threshold” between the two phases, and the system could be driven close  
88 to or beyond this point by an external force; climate change and deforestation are the main forces that could  
89 be the drivers of such a phase change in contemporary forests (Bonan, 2008; Haddad et al., 2015). There  
90 are several applications of this concept in ecology: species' dispersal strategies are influenced by percolation  
91 thresholds in three-dimensional forest structure (Ricard V Solé, Bartumeus, & Gamarra, 2005), and it has  
92 been shown that species distributions also have percolation thresholds (He & Hubbell, 2003). This implies  
93 that pushing the system below the percolation threshold could produce a biodiversity collapse (J. Bascompte  
94 & Solé, 1996; Pardini, Bueno, Gardner, Prado, & Metzger, 2010; Ricard V. Solé, Alonso, & Saldaña, 2004);

95 conversely, being in a connected state (above the threshold) could accelerate the invasion of forest into prairie  
96 (Loehle, Li, & Sundell, 1996; Naito & Cairns, 2015).

97 One of the main challenges with systems that can experience critical transitions—of any kind—is that the  
98 value of the critical threshold is not known in advance. In addition, because near the critical point a small  
99 change can precipitate a state shift of the system, they are difficult to predict. Several methods have been  
100 developed to detect if a system is close to the critical point, e.g. a deceleration in recovery from perturbations,  
101 or an increase in variance in the spatial or temporal pattern (Boettiger & Hastings, 2012; S. R. Carpenter  
102 et al., 2011; Dai, Vorselen, Korolev, & Gore, 2012; Hastings & Wysham, 2010).

103 The existence of a critical transition between two states has been established for forest at global scale in  
104 different works (Hirota, Holmgren, Nes, & Scheffer (2011); Verbesselt et al. (2016); Wuyts, Champneys, &  
105 House (2017)). It was not probed, but is generally believed, that this constitutes a first order catastrophic  
106 transition. The regions where forest can grow are not distributed homogeneously, there are demographic  
107 fluctuations in forest growth and disturbances produced by human activities. Due to new theoretical advances  
108 (Villa Martín, Bonachela, & Muñoz, 2014; Villa Martín et al., 2015) all these factors imply that if these were  
109 first order transitions they will be converted or observed as second order continuous transitions. From this  
110 basis we applied indices derived from second order transitions to global forest cover dynamics.

111 In this study, our objective is to look for evidence that forests around the globe are near continuous critical  
112 point that represent a fragmentation threshold. We use the framework of percolation to first evaluate if  
113 forest patch distribution at a continental scale is described by a power law distribution and then examine  
114 the fluctuations of the largest patch. The advantage of using data at a continental scale is that for very  
115 large systems the transitions are very sharp (R V Solé, 2011) and thus much easier to detect than at smaller  
116 scales, where noise can mask the signals of the transition.

## 117 Methods

### 118 Study areas definition

119 We analyzed mainland forests at a continental scale, covering the whole globe, by delimiting land areas with  
120 a near-contiguous forest cover, separated with each other by large non-forested areas. Using this criterion,  
121 we delimited the following forest regions. In America, three regions were defined: South America temperate  
122 forest (SAT), subtropical and tropical forest up to Mexico (SAST), and USA and Canada forest (NA). Europe  
123 and North Asia were treated as one region (EUAS). The rest of the delimited regions were South-east Asia

124 (SEAS), Africa (AF), and Australia (OC). We also included in the analysis islands larger than  $10^5 \text{ km}^2$ . The  
125 mainland region has the number 1 e.g. OC1, and the nearby islands have consecutive numeration (Appendix  
126 S4, figure S1-S6).

## 127 Forest patch distribution

128 We studied forest patch distribution in each defined area from 2000 to 2015 using the MODerate-resolution  
129 Imaging Spectroradiometer (MODIS) Vegetation Continuous Fields (VCF) Tree Cover dataset version 051  
130 (C. DiMiceli et al., 2015). This dataset is produced at a global level with a 231-m resolution, from 2000  
131 onwards on an annual basis. There are several definition of forest based on percent tree cover (J. O. Sexton  
132 et al., 2015); we choose a range from 20% to 30% threshold in 5% increments to convert the percentage  
133 tree cover to a binary image of forest and non-forest pixels. This range is centered in the definition used by  
134 the United Nations' International Geosphere-Biosphere Programme (Belward, 1996), and studies of global  
135 fragmentation (Haddad et al., 2015) and includes the range used in other studies of critical transitions (C.  
136 Xu et al., 2016). Using this range we try to avoid the errors produced by low discrimination of MODIS VCF  
137 between forest and dense herbaceous vegetation at low forest cover and the saturation of MODIS VCF in  
138 dense forests (J. O. Sexton et al., 2013). We repeat all the analysis described below for this set of thresholds,  
139 except in some specific cases. Patches of contiguous forest were determined in the binary image by grouping  
140 connected forest pixels using a neighborhood of 8 forest units (Moore neighborhood).

## 141 Percolation theory

142 A more in-depth introduction to percolation theory can be found elsewhere (Stauffer & Aharony, 1994) and  
143 a review from an ecological point of view is available (B. Oborny, Szabó, & Meszéna, 2007). Here, to explain  
144 the basic elements of percolation theory we formulate a simple model: we represent our area of interest by a  
145 square lattice and each site of the lattice can be occupied—e.g. by forest—with a probability  $p$ . The lattice  
146 will be more occupied when  $p$  is greater, but the sites are randomly distributed. We are interested in the  
147 connection between sites, so we define a neighborhood as the eight adjacent sites surrounding any particular  
148 site. The sites that are neighbors of other occupied sites define a patch. When there is a patch that connects  
149 the lattice from opposite sides, it is said that the system percolates. When  $p$  is increased from low values, a  
150 percolating patch suddenly appears at some value of  $p$  called the critical point  $p_c$ .

151 Thus percolation is characterized by two well defined phases: the unconnected phase when  $p < p_c$  (called  
152 subcritical in physics), in which species cannot travel far inside the forest, as it is fragmented; in a general

153 sense, information cannot spread. The second is the connected phase when  $p > p_c$  (supercritical), species  
154 can move inside a forest patch from side to side of the area (lattice), i.e. information can spread over the  
155 whole area. Near the critical point several scaling laws arise: the structure of the patch that spans the area  
156 is fractal, the size distribution of the patches is power-law, and other quantities also follow power-law scaling  
157 (Stauffer & Aharony, 1994).

158 The value of the critical point  $p_c$  depends on the geometry of the lattice and on the definition of the  
159 neighborhood, but other power-law exponents only depend on the lattice dimension. Close to the critical  
160 point, the distribution of patch sizes is:

161 (1)  $n_s(p_c) \propto s^{-\alpha}$

162 where  $n_s(p)$  is the number of patches of size  $s$ . The exponent  $\alpha$  does not depend on the details of the  
163 model and it is called universal (Stauffer & Aharony, 1994). These scaling laws can be applied for landscape  
164 structures that are approximately random, or at least only correlated over short distances (Gastner, Oborny,  
165 Zimmermann, & Pruessner, 2009). In physics this is called “isotropic percolation universality class”, and  
166 corresponds to an exponent  $\alpha = 2.05495$ . If we observe that the patch size distribution has another exponent  
167 it will not belong to this universality class and some other mechanism should be invoked to explain it.  
168 Percolation thresholds can also be generated by models that have some kind of memory (Hinrichsen, 2000;  
169 Ódor, 2004): for example, a patch that has been exploited for many years will recover differently than a  
170 recently deforested forest patch. In this case, the system could belong to a different universality class, or in  
171 some cases there is no universality, in which case the value of  $\alpha$  will depend on the parameters and details  
172 of the model (Corrado, Cherubini, & Pennetta, 2014).

173 To illustrate these concepts, we conducted simulations with a simple forest model with only two states: forest  
174 and non-forest. This type of model is called a “contact process” and was introduced for epidemics (Harris,  
175 1974), but has many applications in ecology (Gastner et al., 2009; Ricard V. Solé & Bascompte, 2006). A  
176 site with forest can become extinct with probability  $e$ , and produce another forest site in a neighborhood  
177 with probability  $c$ . We use a neighborhood defined by an isotropic power law probability distribution. We  
178 defined a single control parameter as  $\lambda = c/e$  and ran simulations for the subcritical fragmentation state  
179  $\lambda < \lambda_c$ , with  $\lambda = 2$ , near the critical point for  $\lambda = 2.5$ , and for the supercritical state with  $\lambda = 5$  (see  
180 supplementary data, gif animations).

181 **Patch size distributions**

182 We fitted the empirical distribution of forest patches calculated for each of the thresholds on the range  
183 we previously mentioned. We used maximum likelihood (Clauset, Shalizi, & Newman, 2009; Goldstein,  
184 Morris, & Yen, 2004) to fit four distributions: power-law, power-law with exponential cut-off, log-normal,  
185 and exponential. We assumed that the patch size distribution is a continuous variable that was discretized  
186 by remote sensing data acquisition procedure.

187 We set a minimal patch size ( $X_{min}$ ) at nine pixels to fit the patch size distributions to avoid artifacts at patch  
188 edges due to discretization (Weerman et al., 2012). Besides this hard  $X_{min}$  limit we set due to discretization,  
189 the power-law distribution needs a lower bound for its scaling behavior. This lower bound is also estimated  
190 from the data by maximizing the Kolmogorov-Smirnov (KS) statistic, computed by comparing the empirical  
191 and fitted cumulative distribution functions (Clauset et al., 2009). For the log-normal model we constrain  
192 the values of the  $\mu$  parameter to positive values, this parameter controls the mode of the distribution and  
193 when is negative most of the probability density of the distribution lies outside the range of the forest patch  
194 size data (Limpert, Stahel, & Abbt, 2001).

195 To select the best model we calculated corrected Akaike Information Criteria ( $AIC_c$ ) and Akaike weights for  
196 each model (Burnham & Anderson, 2002). Akaike weights ( $w_i$ ) are the weight of evidence in favor of model  
197  $i$  being the actual best model given that one of the  $N$  models must be the best model for that set of  $N$   
198 models. Additionally, we computed a likelihood ratio test (Clauset et al., 2009; Vuong, 1989) of the power  
199 law model against the other distributions. We calculated bootstrapped 95% confidence intervals (Crawley,  
200 2012) for the parameters of the best model; using the bias-corrected and accelerated (BCa) bootstrap (Efron  
& Tibshirani, 1994) with 10000 replications.

202 **Largest patch dynamics**

203 The largest patch is the one that connects the highest number of sites in the area. This has been used  
204 extensively to indicate fragmentation (R. H. Gardner & Urban, 2007; Ochoa-Quintero et al., 2015). The  
205 relation of the size of the largest patch  $S_{max}$  to critical transitions has been extensively studied in relation  
206 to percolation phenomena (Bazant, 2000; Botet & Ploszajczak, 2004; Stauffer & Aharony, 1994), but seldom  
207 used in ecological studies (for an exception see Gastner et al. (2009)). When the system is in a connected  
208 state ( $p > p_c$ ) the landscape is almost insensitive to the loss of a small fraction of forest, but close to the  
209 critical point a minor loss can have important effects (B. Oborny et al., 2007; Ricard V. Solé & Bascompte,  
210 2006), because at this point the largest patch will have a filamentary structure, i.e. extended forest areas

211 will be connected by thin threads. Small losses can thus produce large fluctuations.

212 One way to evaluate the fragmentation of the forest is to calculate the proportion of the largest patch against  
213 the total area (Keitt, Urban, & Milne, 1997). The total area of the regions we are considering (Appendix S4,  
214 figures S1-S6) may not be the same than the total area that the forest could potentially occupy, thus a more  
215 accurate way to evaluate the weight of  $S_{max}$  is to use the total forest area, that can be easily calculated  
216 summing all the forest pixels. We calculate the proportion of the largest patch for each year, dividing  $S_{max}$   
217 by the total forest area of the same year:  $RS_{max} = S_{max}/\sum_i S_i$ . This has the effect of reducing the  $S_{max}$   
218 fluctuations produced due to environmental or climatic changes influences in total forest area. When the  
219 proportion  $RS_{max}$  is large (more than 60%) the largest patch contains most of the forest so there are fewer  
220 small forest patches and the system is probably in a connected phase. Conversely, when it is low (less than  
221 20%), the system is probably in a fragmented phase (Saravia & Momo, 2017). As we calculated these largest  
222 patch indices for different thresholds, the values of the total forest area and the value of  $S_{max}$  are lower as  
223 threshold is higher, we expect that the value of  $RS_{max}$  will change and probably be lower at high thresholds.  
224 To define if a region will be in a connected or unconnected state we used the  $RS_{max}$  of the highest threshold  
225 (40%) which is more conservative to evaluate the risk of fragmentation and includes the most dense forest  
226 area. Additionally if  $RS_{max}$  is a good indicator of the fragmented or unfragmented state of the forest and  
227 these are the two alternative states for the critical transition the  $RS_{max}$  distribution of frequencies should be  
228 bimodal (Brandon T. Bestelmeyer et al., 2011); so we apply the Hartigan's dip test that measures departures  
229 from unimodality (J. A. Hartigan & Hartigan, 1985).

230 The  $RS_{max}$  is a useful qualitative index that does not tell us if the system is near or far from the critical  
231 transition; this can be evaluated using the temporal fluctuations. We calculate the fluctuations around the  
232 mean with the absolute values  $\Delta S_{max} = S_{max}(t) - \langle S_{max} \rangle$ , using the proportions of  $RS_{max}$ . To characterize  
233 fluctuations we fitted three empirical distributions: power-law, log-normal, and exponential, using the same  
234 methods described previously. We expect that large fluctuation near a critical point have heavy tails (log-  
235 normal or power-law) and that fluctuations far from a critical point have exponential tails, corresponding to  
236 Gaussian processes (Rooij, Nash, Rajaraman, & Holden, 2013). As the data set spans 16 years, it is probable  
237 that will do not have enough power to reliably detect which distribution is better (Clauset et al., 2009). To  
238 improve this we used the same likelihood ratio test we used previously (Clauset et al., 2009; Vuong, 1989);  
239 if the p-value obtained to compare the best distribution against the others we concluded that there is not  
240 enough data to decide which is the best model. We generated animated maps showing the fluctuations of  
241 the two largest patches at 30% threshold, to aid in the interpretations of the results.

242 A robust way to detect if the system is near a critical transition is to analyze the increase in variance of

the density (Benedetti-Cecchi, Tamburello, Maggi, & Bulleri, 2015). It has been demonstrated that the variance increase in density appears when the system is very close to the transition (Corrado et al., 2014), thus practically it does not constitute an early warning indicator. An alternative is to analyze the variance of the fluctuations of the largest patch  $\Delta S_{max}$ : the maximum is attained at the critical point but a significant increase occurs well before the system reaches the critical point (Corrado et al., 2014; Saravia & Momo, 2017). In addition, before the critical fragmentation, the skewness of the distribution of  $\Delta S_{max}$  should be negative, implying that fluctuations below the average are more frequent. We characterized the increase in the variance using quantile regression: if variance is increasing the slopes of upper or/and lower quartiles should be positive or negative.

All statistical analyses were performed using the GNU R version 3.3.0 (R Core Team, 2015), to fit the distributions of patch sizes we used the Python package powerlaw (Alstott, Bullmore, & Plenz, 2014). For the quantile regressions we used the R package quantreg (Koenker, 2016). Image processing was done in MATLAB r2015b (The Mathworks Inc.). The complete source code for image processing and statistical analysis, and the patch size data files are available at figshare <http://dx.doi.org/10.6084/m9.figshare.4263905>.

## Results

The figure 1 shows an example of the distribution of the biggest 200 patches for years 2000 and 2014, this distribution is highly variable, but the biggest patch usually maintains its place. Sometimes the biggest patch breaks and then big fluctuations in its size are observed, as we will analyze below. Smaller patches can merge or break more easily so they enter or leave the list of 200, and this is why there is a color change across years.

The power law distribution was selected as the best model in 99% of the cases (Figure S7). In a small number of cases (1%) the power law with exponential cutoff was selected, but the value of the parameter  $\alpha$  was similar by  $\pm 0.03$  to the pure power law (Table S1, and model fit data table). Additionally the patch size where the exponential tail begins is very large, thus we used the power law parameters for this cases (region EUAS3,SAST2). In finite-size systems the favored model should be the power law with exponential cut-off, because the power-law tails are truncated to the size of the system (Stauffer & Aharony, 1994). This implies that differences between the two kinds of power law models should be small. We observed that phenomena: when the pure power-law model is selected as the best model the likelihood ratio test shows that in 64% of the cases the differences with power law with exponential cutoff are not significant ( $p\text{-value}>0.05$ ); in these cases the differences between the fitted  $\alpha$  for both models are less than 0.001. Instead the likelihood ratio

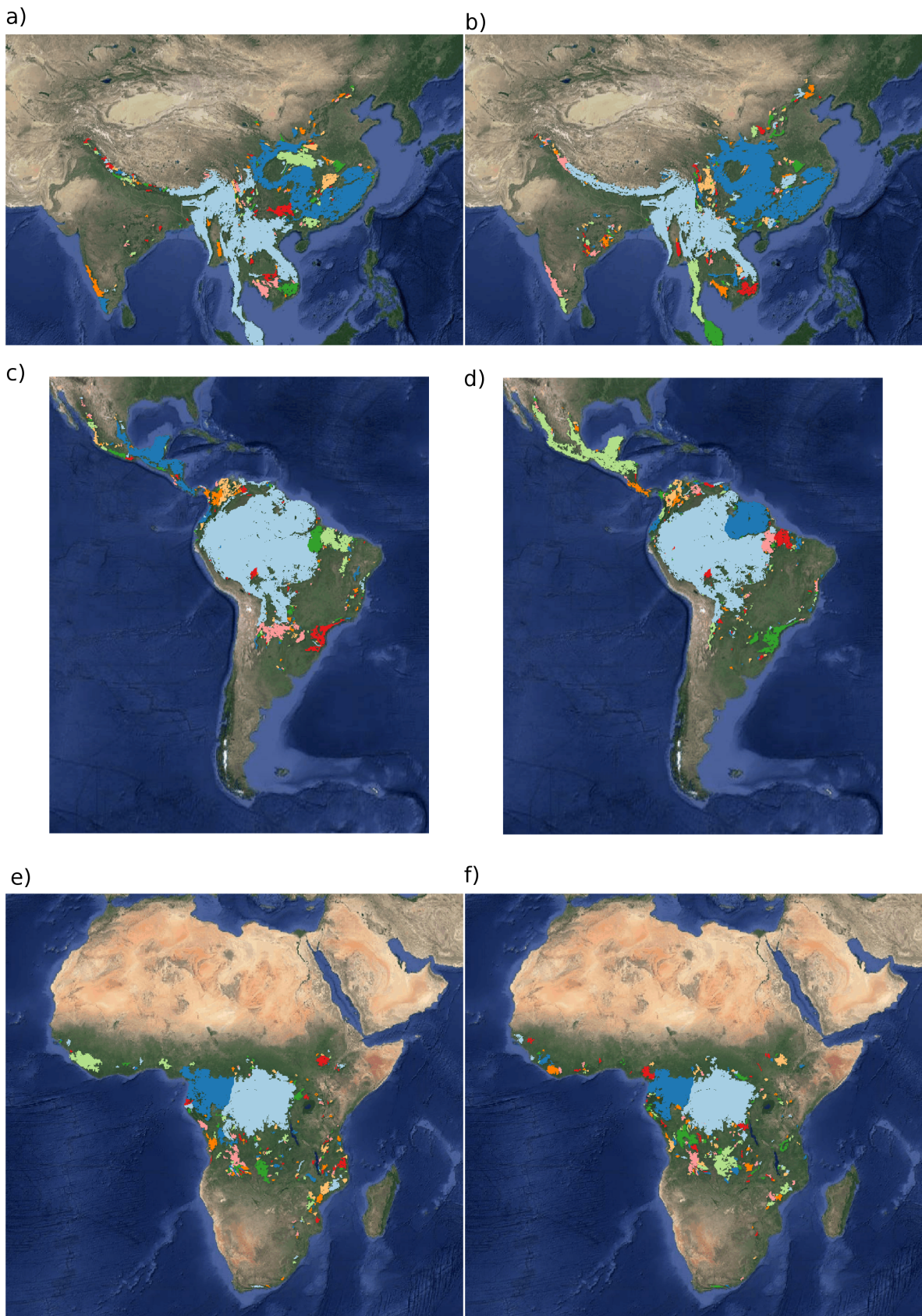


Figure 1: Forest patch distributions for continental regions for the years 2000 and 2014. The images are the 200 biggest patches, showed at a coarse pixel scale of 2.5 Km. The regions are: a) & b) southeast Asia; c) & d) South America subtropical and tropical and e) & f) Africa mainland, for the years 2000 and 2014 respectively. The color palette was chosen to discriminate different patches and do not represent patch size.

273 test clearly differentiates the power law model from the exponential model (100% cases p-value<0.05), and  
274 the log-normal model (90% cases p-value<0.05).

275 The global mean of the power-law exponent  $\alpha$  is 1.967 and the bootstrapped 95% confidence interval is 1.964  
276 - 1.970. Besides that, the global values for each threshold are different, because their confidence intervals  
277 do not overlap, and their range goes from 1.90 to 2.00 (Table S1). Analyzing the biggest regions (Figure  
278 1, Table S2) the north hemisphere (EUAS1 & NA1) have similar values of  $\alpha$  (1.97, 1.98), pantropical areas  
279 have different  $\alpha$  with greatest values for South America (SAST1, 2.01) and in descending order Africa (AF1,  
280 1.946) and Southeast Asia (SEAS1, 1.895). With greater  $\alpha$  the fluctuations of patch sizes are lower and vice  
281 versa (M. E. J. Newman, 2005).

282 We calculated the total areas of forest and the largest patch  $S_{max}$  by year for different thresholds; as expected  
283 these two values increase for smaller thresholds (Table S3). We expect less variations in the largest patch  
284 relative to total forest area  $RS_{max}$  (Figure S9); in ten cases it keeps near or higher than 60% (EUAS2, NA5,  
285 OC2, OC3, OC4, OC5, OC6, OC8, SAST1, SAT1) over the 25-35 range or more. In four cases it keeps  
286 around 40% or less at least over the 25-30% range (AF1, EUAS3, OC1, SAST2) and in six cases there is  
287 a crossover from more than 60% to around 40% or less (AF2, EUAS1, NA1, OC7, SEAS1, SEAS2). This  
288 confirms the criteria of using the most conservative threshold value of 40% to interpret  $RS_{max}$  with regard  
289 to the fragmentation state of the forest. The frequency of  $RS_{max}$  showed bimodality (Figure 3) and the dip  
290 test rejected unimodality ( $D = 0.0416$ , p-value = 0.0003), which also indicates  $RS_{max}$  as a good index to  
291 study the fragmentation state of the forest.

292 The  $RS_{max}$  for regions with more than  $10^7$  km<sup>2</sup> of forest is shown in figure 4. South America tropical and  
293 subtropical (SAST1) is the only region with an average close to 60%, the other regions are below 30%. Eurasia  
294 mainland (EUAS1) has the lowest value near 20%. For regions with less total forest area (Figure S10, Table  
295 S3), Great Britain (EUAS3) has the lowest proportion less than 5%, Java (OC7) and Cuba (SAST2) are  
296 under 25%, while other regions such as New Guinea (OC2), Malaysia/Kalimantan (OC3), Sumatra (OC4),  
297 Sulawesi (OC5) and South New Zealand (OC6) have a very high proportion (75% or more). Philippines  
298 (SEAS2) seems to be a very interesting case because it seems to be under 30% until the year 2007, fluctuates  
299 around 30% in years 2008-2010, then jumps near 60% in 2011-2013 and then falls again to 30%, this seems  
300 an example of a transition from a fragmented state to a unfragmented one (figure S10).

301 We analyzed the distributions of fluctuations of the largest patch relative to total forest area  $\Delta RS_{max}$  and  
302 the fluctuations of the largest patch  $\Delta S_{max}$ . Besides the Akaike criteria identified different distributions as  
303 the best, in most cases the Likelihood ratio test is not significant thus the data is not enough to determine

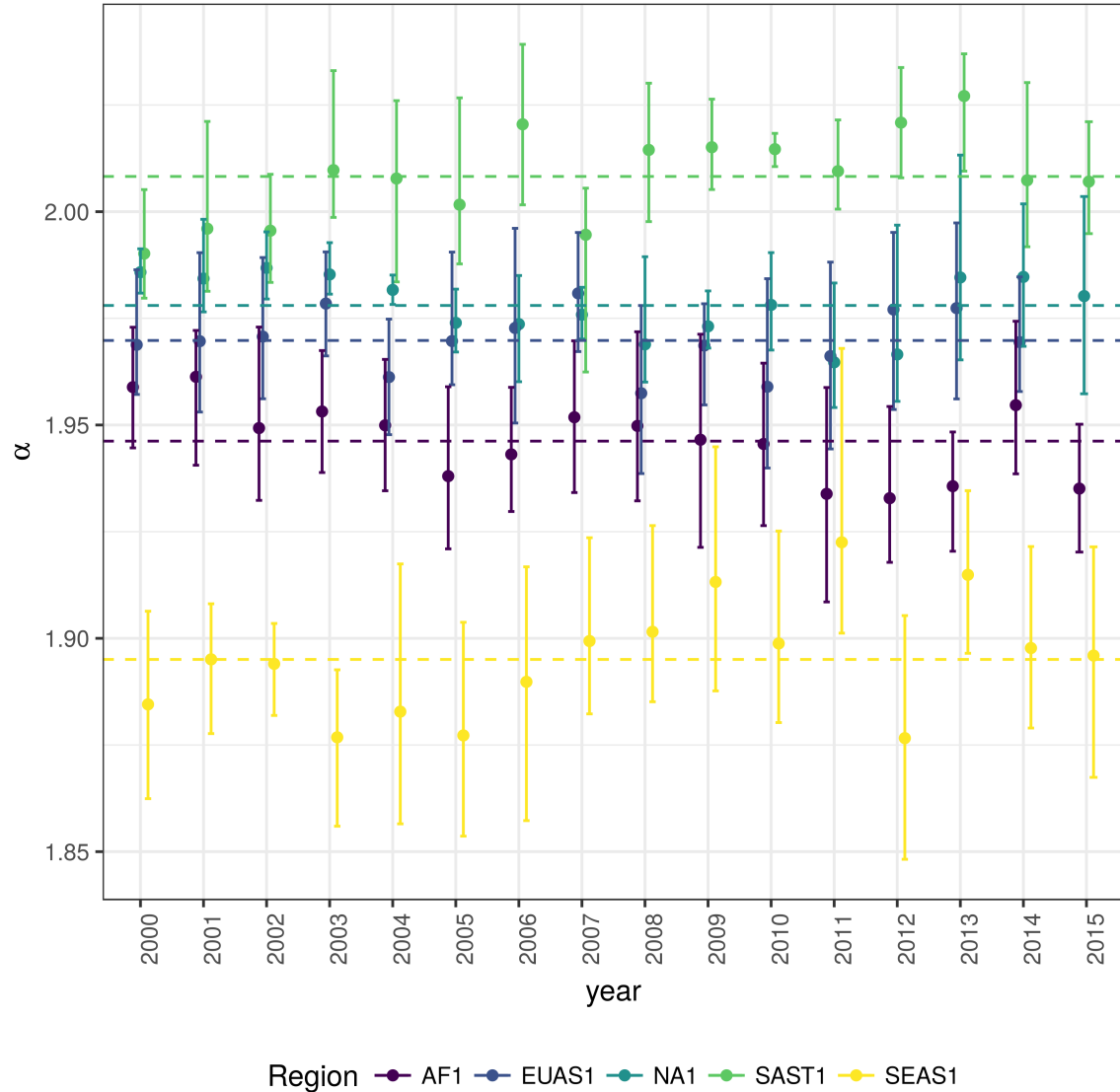


Figure 2: Power law exponents ( $\alpha$ ) of forest patch distributions for regions with total forest area  $> 10^7 \text{ km}^2$ . Dashed horizontal lines are the means by region, with 95% confidence interval error bars estimated by bootstrap resampling. The regions are AF1: Africa mainland, EUAS1: Eurasia mainland, NA1: North America mainland, SAST1: South America subtropical and tropical, SEAS1: Southeast Asia mainland.

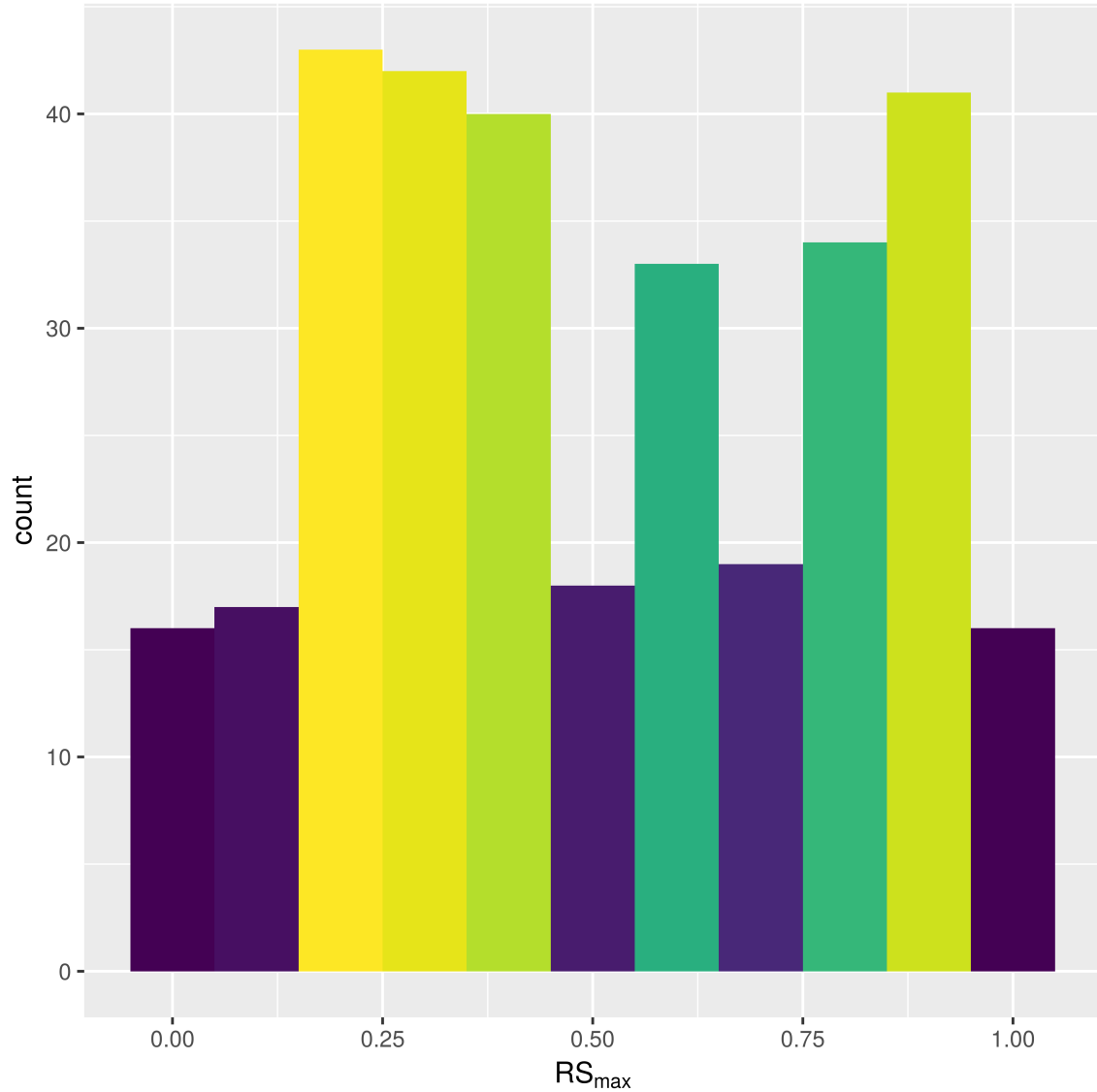


Figure 3: Frequency distribution of Largest patch proportion relative to total forest area  $RS_{max}$  calculated using a threshold of 40% of forest in each pixel to determine patches. Bimodality is observed and confirmed by the dip test ( $D = 0.0416$ ,  $p\text{-value} = 0.0003$ ). This indicates the existence of two states needed for a critical transition.

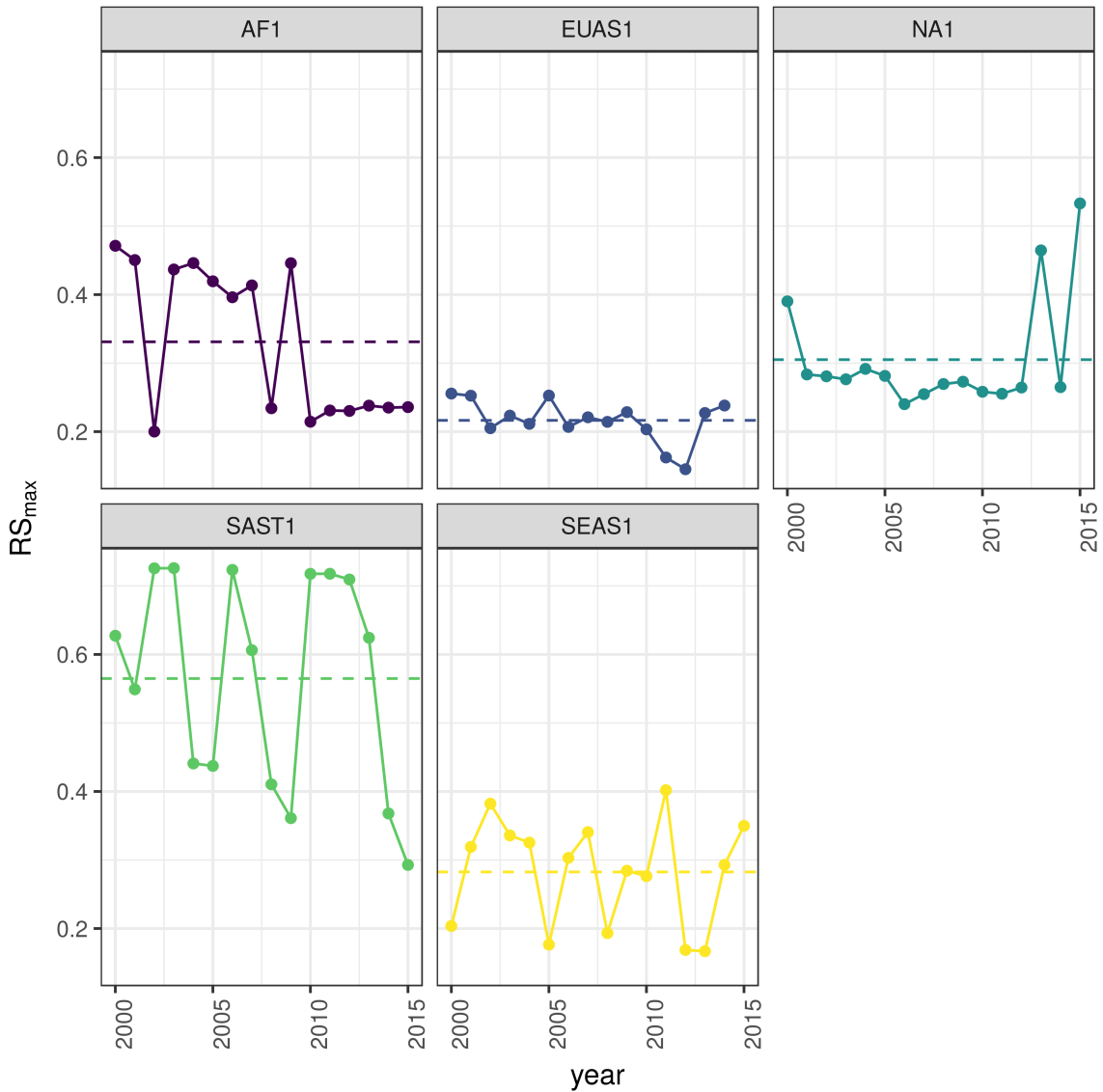


Figure 4: Largest patch proportion relative to total forest area  $RS_{max}$ , for regions with total forest area  $> 10^7 \text{ km}^2$ . We show here the  $RS_{max}$  calculated using a threshold of 40% of forest in each pixel to determine patches. Dashed lines are averages across time. The regions are AF1: Africa mainland, EUAS1: Eurasia mainland, NA1: North America mainland, SAST1: South America tropical and subtropical, SEAS1: Southeast Asia mainland.

304 with confidence which is the best distribution. Only 1 case the distribution selected by the Akaike criteria is  
305 confirmed as the correct model for relative and absolute fluctuations (Table S4). Thus we do not apply this  
306 criteria because is not informative, we can not decide with reliability if the best distribution is the selected  
307 one.

308 The animations of the two largest patches (see supplementary data, largest patch gif animations) qualitatively  
309 shows the nature of fluctuations and if the state of the forest is connected or not. If the largest patch is  
310 always the same patch over time, the forest is probably not fragmented; this happens for regions with  $RS_{max}$   
311 of more than 40% such as AF2 (Madagascar), EUAS2 (Japan), NA5 (Newfoundland) and OC3 (Malaysia).  
312 In the regions with  $RS_{max}$  between 40% and 30% the identity of the largest patch could change or stay the  
313 same in time. For OC7 (Java) the largest patch changes and for AF1 (Africa mainland) it stays the same.  
314 Only for EUAS1 (Eurasia mainland) we observed that the two largest patches are always the same, implying  
315 that this region is probably composed of two independent domains and should be divided in further studies.  
316 The regions with  $RS_{max}$  less than 25%: SAST2 (Cuba) and EUAS3 (Great Britain), the largest patch always  
317 changes reflecting their fragmented state. In the case of SEAS2 (Philippines) a transition is observed, with  
318 the identity of the largest patch first variable, and then constant after 2010.

319 The results of quantile regressions are almost identical for  $\Delta RS_{max}$  and  $\Delta S_{max}$  (table S5). Among the  
320 biggest regions, Africa (AF1) has upper and lower quantiles with significantly negative slopes, but the lower  
321 quantile slope is lower, implying that negative fluctuations and variance are increasing (Figure 5). Eurasia  
322 mainland (EUAS1) has only the upper quantile significant with a positive slope, suggesting an increase in the  
323 variance. North America mainland (NA1) exhibits a significant lower quantile with positive slope, implying  
324 decreasing variance. Finally, for mainland Australia, all quantiles are significant, and the slope of the lower  
325 quantiles is greater than the upper ones, showing that variance is decreasing (Appendix S4, figure S10).  
326 These results are summarized in Table 1.

327 The conditions that indicate that a region is near a critical fragmentation threshold are that patch size  
328 distributions follow a power law; temporal  $\Delta RS_{max}$  fluctuations follow a power law; variance of  $\Delta RS_{max}$  is  
329 increasing in time; and skewness is negative. All these conditions were true only for Africa mainland (AF1)  
330 and South America tropical & subtropical (SAST1).

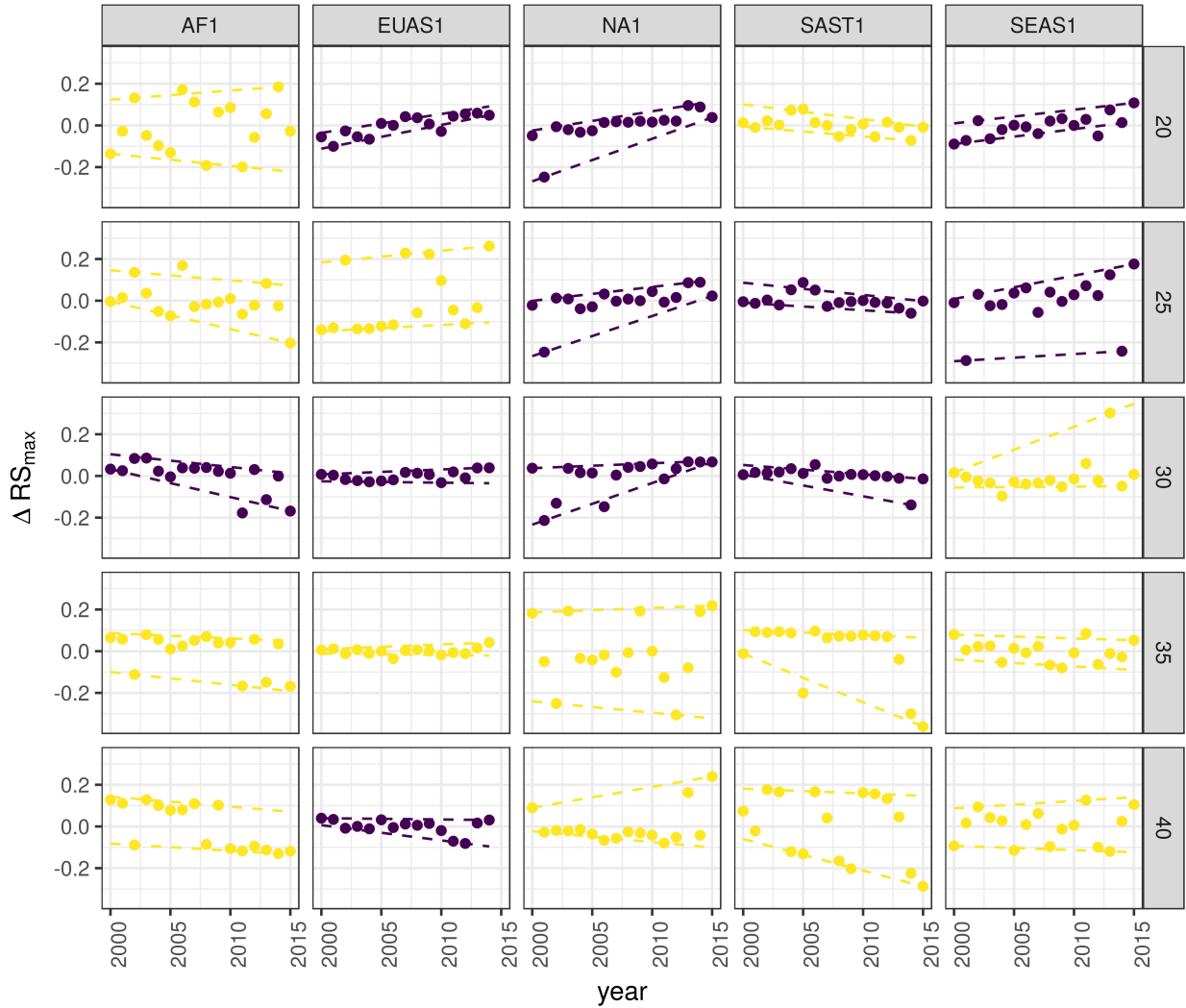


Figure 5: Largest patch fluctuations for regions with total forest area  $> 10^7 \text{ km}^2$  across years. The patch sizes are relative to the total forest area of the same year. Dashed lines are 90%, 50% and 10% quantile regressions, to show if fluctuations were increasing. The regions are AF1: Africa mainland, EUAS1: Eurasia mainland, NA1: North America mainland, SAST1: South America tropical and subtropical, SEAS1: Southeast Asia mainland.

Table 1: Regions and indicators of closeness to a critical fragmentation threshold. Where,  $RS_{max}$  is the largest patch divided by the total forest area,  $\Delta RS_{max}$  are the fluctuations of  $RS_{max}$  around the mean, skewness was calculated for  $RS_{max}$  and the increase or decrease in the variance was estimated using quantile regressions, NS means the results were non-significant. The conditions that determine the closeness to a threshold are: power law distributions in patch sizes and  $\Delta RS_{max}$ ; increasing variance of  $\Delta RS_{max}$  and negative skewness.

| Region | Description              | Variance of |           |                   |          |
|--------|--------------------------|-------------|-----------|-------------------|----------|
|        |                          | $RS_{max}$  | Threshold | $\Delta RS_{max}$ | Skewness |
| AF1    | Africa mainland          | 0.33        | 30        | Increase          | -1.4653  |
| AF2    | Madagascar               | 0.48        | 20        | Increase          | 0.7226   |
| EUAS1  | Eurasia, mainland        | 0.22        | 20        | Decrease          | -0.4814  |
| EUAS1  |                          |             | 30        | Increase          | 0.3113   |
| EUAS1  |                          |             | 40        | Increase          | -1.2790  |
| EUAS2  | Japan                    | 0.94        | 35        | Increase          | -0.3913  |
| EUAS2  |                          |             | 40        | Increase          | -0.5030  |
| EUAS3  | Great Britain            | 0.03        | 40        | NS                |          |
| NA1    | North America, mainland  | 0.31        | 20        | Decrease          | -2.2895  |
| NA1    |                          |             | 25        | Decrease          | -2.4465  |
| NA1    |                          |             | 30        | Decrease          | -1.6340  |
| NA5    | Newfoundland             | 0.54        | 40        | NS                |          |
| OC1    | Australia, Mainland      | 0.36        | 30        | Increase          | 0.0920   |
| OC1    |                          |             | 35        | Increase          | -0.8033  |
| OC2    | New Guinea               | 0.96        | 25        | Decrease          | -0.1003  |
| OC2    |                          |             | 30        | Decrease          | 0.1214   |
| OC2    |                          |             | 35        | Decrease          | -0.0124  |
| OC3    | Malaysia/Kalimantan      | 0.92        | 35        | Increase          | -1.0147  |
| OC3    |                          |             | 40        | Increase          | -1.5649  |
| OC4    | Sumatra                  | 0.84        | 20        | Increase          | -1.3846  |
| OC4    |                          |             | 25        | Increase          | -0.5887  |
| OC4    |                          |             | 30        | Increase          | -1.4226  |
| OC5    | Sulawesi                 | 0.82        | 40        | NS                |          |
| OC6    | New Zealand South Island | 0.75        | 40        | Increase          | 0.3553   |
| OC7    | Java                     | 0.16        | 40        | NS                |          |

| Region | Description   | $RS_{max}$ | Threshold | Variance of       |          |
|--------|---|------------|-----------|-------------------|----------|
|        |   |            |           | $\Delta RS_{max}$ | Skewness |
| OC8    | New Zealand North Island                                    | 0.64       | 40        | NS                |          |
| SAST1  | South America, Tropical and Subtropical forest up to Mexico | 0.56       | 25        | Increase          | 1.0519   |
| SAST1  |   |            | 30        | Increase          | -2.7216  |
| SAST2  | Cuba  | 0.15       | 20        | Increase          | 0.5049   |
| SAST2  |   |            | 25        | Increase          | 1.7263   |
| SAST2  |   |            | 30        | Increase          | 0.1665   |
| SAST2  |   |            | 40        | Increase          | -0.5401  |
| SAT1   | South America, Temperate forest                             | 0.54       | 25        | Decrease          | 0.1483   |
| SAT1   |   |            | 30        | Decrease          | -1.6059  |
| SAT1   |   |            | 35        | Decrease          | -1.3809  |
| SEAS1  | outheast Asia, Mainland S                                   | 0.28       | 25        | Increase          | -1.3328  |
| SEAS2  | hilippines P  | 0.33       | 20        | Decrease          | -1.6373  |
| SEAS2  |   |            | 25        | Decrease          | -0.6648  |
| SEAS2  |   |            | 30        | Increase          | 0.1517   |
| SEAS2  |   |            | 40        | Increase          | 1.5996   |

## 331 Discussion

332 We found that the forest patch distribution of most regions of the world followed power laws spanning  
 333 seven orders of magnitude. These include tropical rainforest, boreal and temperate forest. Power laws have  
 334 previously been found for several kinds of vegetation, but never at global scales as in this study. Interestingly,  
 335 Eurasia does not follow a power law, but it is a geographically extended region, consisting of different domains  
 336 (as we observed in the largest patch animations, see supplementary data). It is known that the union of two  
 337 independent power law distributions produces a lognormal distribution (Rooij et al., 2013). Future studies  
 338 should split this region into two or more new regions, and test if the underlying distributions are power laws.

339 Several mechanisms have been proposed for the emergence of power laws in forest: the first is related self  
340 organized criticality (SOC), when the system is driven by its internal dynamics to a critical state; this has  
341 been suggested mainly for fire-driven forests (Hantson, Pueyo, & Chuvieco, 2015; Zinck & Grimm, 2009).  
342 Real ecosystems do not seem to meet the requirements of SOC dynamics (McKenzie & Kennedy, 2012; S.  
343 Pueyo et al., 2010; Sole, Alonso, & Mckane, 2002). A second possible mechanism, suggested by Pueyo  
344 et al. (2010), is isotropic percolation, when a system is near the critical point power law structures arise.  
345 This is equivalent to the random forest model that we explained previously, and requires the tuning of an  
346 external environmental condition to carry the system to this point. We did not expect forest growth to be a  
347 random process at local scales, but it is possible that combinations of factors cancel out to produce seemingly  
348 random forest dynamics at large scales. If this is the case the power law exponent should be theoretically  
349 near  $\alpha = 2.055$ ; this is close but outside the confidence interval we observed (1.898 - 1.920). The third  
350 mechanism suggested as the cause of pervasive power laws in patch size distribution is facilitation (Irvine,  
351 Bull, & Keeling, 2016; Manor & Shnerb, 2008): a patch surrounded by forest will have a smaller probability  
352 of being deforested or degraded than an isolated patch. We hypothesize that models that include facilitation  
353 could explain the patterns observed here. The model of Scanlon et al. (2007) showed an  $\alpha = 1.34$  which  
354 is also different from our results. Another model but with three states (tree/non-tree/degraded), including  
355 local facilitation and grazing, was also used to obtain power laws patch distributions without external tuning,  
356 and exhibited deviations from power laws at high grazing pressures (S. Kéfi et al., 2007). The values of the  
357 power law exponent  $\alpha$  obtained for this model are dependent on the intensity of facilitation, when facilitation  
358 is more intense the exponent is higher, but the maximal values they obtained are still lower than the ones  
359 we observed. The interesting point is that the value of the exponent is dependent on the parameters, and  
360 thus the observed  $\alpha$  might be obtained with some parameter combination.

361 It has been suggested that a combination of spatial and temporal indicators could more reliably detect  
362 critical transitions (S. Kéfi et al., 2014). In this study, we combined five criteria to detect the closeness to  
363 a fragmentation threshold. Two of them were spatial: the forest patch size distribution, and the proportion  
364 of the largest patch relative to total forest area ( $RS_{max}$ ). The other three were the distribution of temporal  
365 fluctuations in the largest patch size, the trend in the variance, and the skewness of the fluctuations. Each  
366 one of these is not a strong individual predictor, but their combination gives us an increased degree of  
367 confidence about the system being close to a critical transition.

368 We found that only the tropical forest of Africa and South America met all five criteria, and thus seem to be  
369 near a critical fragmentation threshold. This confirms previous studies that point to these two tropical areas  
370 as the most affected by deforestation (M. C. Hansen et al., 2013). Africa seems to be more affected, because

371 the proportion of the largest patch relative to total forest area ( $RS_{max}$ ) is near 30%, which could indicate  
372 that the transition is already started. Moreover, this region was estimated to be potentially bistable, with  
373 the possibility to completely transform into a savanna (Staver, Archibald, & Levin, 2011). The main driver  
374 of deforestation in this area was smallholder farming.

375 The region of South America tropical forest has a  $RS_{max}$  of more than 60%, suggesting that the fragmentation  
376 transition is approaching but not yet started. In this region, a striking decline in deforestation rates has  
377 been observed in Brasil, which hosts most of the biggest forest patch, but deforestation rates have continued  
378 to increase in surrounding countries (Argentina, Paraguay, Bolivia, Colombia, Peru) thus the region is still  
379 at a high risk.

380 The monitoring of biggest patches is also important because they contain most of the intact forest landscapes  
381 defined by P. Potapov et al. (2008), thus a relatively simple way to evaluate the risk in these areas is to  
382 use  $RS_{max}$  index. The analysis of  $RS_{max}$  reveals that the island of Philippines (SEAS2) seems to be an  
383 example of a critical transition from an unconnected to a connected state, the early warning signals can  
384 be qualitatively observed: a big fluctuation in a negative direction precedes the transition and then  $RS_{max}$   
385 stabilizes over 60% (Figure S9). In addition, there was a total loss of forest cover of 1.9% from year 2000 to  
386 2012 (M. C. Hansen et al., 2013) and deforestation rates were not substantially reduced in 1990-2014; this  
387 could be the results of an active intervention of the government promoting conservation and rehabilitation  
388 of protected areas, ban of logging old-growth forest, reforestation of barren areas, community-based forestry  
389 activities, and sustainable forest management in the country's production forest (Lasco et al., 2008). This  
390 confirms that the early warning indicators proposed here work in the correct direction.

391 The region of Southeast Asia was also one of the most deforested places in the world, but was not detected  
392 as a region near a fragmentation threshold. This is probably due to the forest conservation and restoration  
393 programs implemented by the Chinese government, which bans logging in natural forests and monitor illegal  
394 harvesting (Viña, McConnell, Yang, Xu, & Liu, 2016). The MODIS dataset does not detect if native forest  
395 is replaced by agroindustrial tree plantations like oil palms, that are among the main drivers of deforestation  
396 in this area (Malhi, Gardner, Goldsmith, Silman, & Zelazowski, 2014). To improve the estimation of forest  
397 patches, data sets as the MODIS cropland probability and others about land use, protected areas, forest  
398 type, should be incorporated (M. Hansen et al., 2014; J. O. Sexton et al., 2015).

399 Deforestation and fragmentation are closely related. At low levels of habitat reduction species population  
400 will decline proportionally; this can happen even when the habitat fragments retain connectivity. As habi-  
401 tation reduction continues, the critical threshold is approached and connectivity will have large fluctuations

402 (Brook, Ellis, Perring, Mackay, & Blomqvist, 2013). This could trigger several negative synergistic effects:  
403 populations fluctuations and the possibility of extinctions will rise, increasing patch isolation and decreasing  
404 connectivity (Brook et al., 2013). This positive feedback mechanism will be enhanced when the fragmenta-  
405 tion threshold is reached, resulting in the loss of most habitat specialist species at a landscape scale (Pardini  
406 et al., 2010). Some authors argue that since species have heterogeneous responses to habitat loss and frag-  
407 mentation, and biotic dispersal is limited, the importance of thresholds is restricted to local scales or even  
408 that its existence is questionable (Brook et al., 2013). Fragmentation is by definition a local process that at  
409 some point produces emergent phenomena over the entire landscape, even if the area considered is infinite  
410 (B. Oborny, Meszéna, & Szabó, 2005). In addition, after a region's fragmentation threshold connectivity  
411 decreases, there is still a large and internally well connected patch that can maintain sensitive species (A. C.  
412 Martensen, Ribeiro, Banks-Leite, Prado, & Metzger, 2012). What is the time needed for these large patches  
413 to become fragmented, and pose a real danger of extinction to a myriad of sensitive species? If a forest is  
414 already in a fragmented state, a second critical transition from forest to non-forest could happen, this was  
415 called the desertification transition (Corrado et al., 2014). Considering the actual trends of habitat loss,  
416 and studying the dynamics of non-forest patches—instead of the forest patches as we did here—the risk of  
417 this kind of transition could be estimated. The simple models proposed previously could also be used to  
418 estimate if these thresholds are likely to be continuous and reversible or discontinuous and often irreversible  
419 (Weissmann & Shnerb, 2016), and the degree of protection (e.g. using the set-asides strategy Banks-Leite et  
420 al. (2014)) than would be necessary to stop this trend.

421 The effectiveness of landscape management is related to the degree of fragmentation, and the criteria to  
422 direct reforestation efforts could be focused on regions near a transition (B. Oborny et al., 2007). Regions  
423 that are in an unconnected state require large efforts to recover a connected state, but regions that are near  
424 a transition could be easily pushed to a connected state; feedbacks due to facilitation mechanisms might  
425 help to maintain this state. Crossing the fragmentation critical point in forests could have negative effects  
426 on biodiversity and ecosystem services (Haddad et al., 2015), but it could also produce feedback loops at  
427 different levels of the biological hierarchy. This means that a critical transition produced at a continental  
428 scale could have effects at the level of communities, food webs, populations, phenotypes and genotypes  
429 (Barnosky et al., 2012). All these effects interact with climate change, thus there is a potential production of  
430 cascading effects that could lead to a global collapse. Therefore, even if critical thresholds are reached only in  
431 some forest regions at a continental scale, a cascading effect with global consequences could still be produced,  
432 and may contribute to reach a planetary tipping point (Reyer, Rammig, Brouwers, & Langerwisch, 2015).  
433 The risk of such event will be higher if the dynamics of separate continental regions are coupled (Lenton &

<sup>434</sup> Williams, 2013). Using the time series obtained in this work the coupling of the continental could be further  
<sup>435</sup> investigated. It has been proposed that to assess the probability of a global scale shift, different small scale  
<sup>436</sup> ecosystems should be studied in parallel (Barnosky et al., 2012). As forest comprises a major proportion  
<sup>437</sup> of such ecosystems, we think that the transition of forests could be used as a proxy for all the underling  
<sup>438</sup> changes and as a successful predictor of a planetary tipping point.

## <sup>439</sup> Supporting information

### <sup>440</sup> Appendix

<sup>441</sup> *Table S1:* Proportion of Power law models not rejected by the goodness of fit test at  $p \leq 0.05$  level.

<sup>442</sup> *Table S2:* Generalized least squares fit by maximizing the restricted log-likelihood.

<sup>443</sup> *Table S3:* Simultaneous Tests for General Linear Hypotheses of the power law exponent.

<sup>444</sup> *Table S4:* Quantile regressions of the proportion of largest patch area vs year.

<sup>445</sup> *Table S5:* Unbiased estimation of skewness for absolute largest patch fluctuations and relative fluctuations.

<sup>446</sup> *Table S6:* Model selection using Akaike criterion for largest patch fluctuations in absolute values

<sup>447</sup> *Table S7:* Model selection for fluctuation of largest patch in relative to total forest area.

<sup>448</sup> *Figure S1:* Regions for Africa (AF), 1 Mainland, 2 Madagascar.

<sup>449</sup> *Figure S2:* Regions for Eurasia (EUAS), 1 Mainland, 2 Japan, 3 Great Britain.

<sup>450</sup> *Figure S3:* Regions for North America (NA), 1 Mainland, 5 Newfoundland.

<sup>451</sup> *Figure S4:* Regions for Australia and islands (OC), 1 Australia mainland; 2 New Guinea; 3 Malaysia/Kalimantan;  
<sup>452</sup> 4 Sumatra; 5 Sulawesi; 6 New Zealand south island; 7 Java; 8 New Zealand north island.

<sup>453</sup> *Figure S5:* Regions for South America, SAST1 Tropical and subtropical forest up to Mexico; SAST2 Cuba;  
<sup>454</sup> SAT1 South America, Temperate forest.

<sup>455</sup> *Figure S6:* Regions for Southeast Asia (SEAS), 1 Mainland; 2 Philippines.

<sup>456</sup> *Figure S7:* Proportion of best models selected for patch size distributions using the Akaike criterion.

<sup>457</sup> *Figure S8:* Power law exponents for forest patch distributions by year.

<sup>458</sup> *Figure S9:* Largest patch proportion relative to total forest area  $RS_{max}$ , for regions with total forest area  
<sup>459</sup> less than  $10^7 \text{ km}^2$ .

<sup>460</sup> *Figure S10:* Fluctuations of largest patch for regions with total forest area less than  $10^7$  km<sup>2</sup>. The patch  
<sup>461</sup> sizes are relativized to the total forest area for that year.

## <sup>462</sup> Data Accessibility

<sup>463</sup> Csv text file with model fits for patch size distribution, and model selection for all the regions; Gif Animations  
<sup>464</sup> of a forest model percolation; Gif animations of largest patches; patch size files for all years and regions  
<sup>465</sup> used here; and all the R and Matlab scripts are available at figshare <http://dx.doi.org/10.6084/m9.figshare.4263905>.

## <sup>467</sup> Acknowledgments

<sup>468</sup> LAS and SRD are grateful to the National University of General Sarmiento for financial support. This work  
<sup>469</sup> was partially supported by a grant from CONICET (PIO 144-20140100035-CO).

## <sup>470</sup> References

- <sup>471</sup> Allington, G. R. H., & Valone, T. J. (2010). Reversal of desertification: The role of physical and chemical  
<sup>472</sup> soil properties. *Journal of Arid Environments*, 74(8), 973–977. doi:10.1016/j.jaridenv.2009.12.005
- <sup>473</sup> Alstott, J., Bullmore, E., & Plenz, D. (2014). powerlaw: A Python Package for Analysis of Heavy-Tailed  
<sup>474</sup> Distributions. *PLOS ONE*, 9(1), e85777. Retrieved from <https://doi.org/10.1371/journal.pone.0085777>
- <sup>475</sup> Banks-Leite, C., Pardini, R., Tambosi, L. R., Pearse, W. D., Bueno, A. A., Bruscagin, R. T., ... Metzger,  
<sup>476</sup> J. P. (2014). Using ecological thresholds to evaluate the costs and benefits of set-asides in a biodiversity  
<sup>477</sup> hotspot. *Science*, 345(6200), 1041–1045. doi:10.1126/science.1255768
- <sup>478</sup> Barnosky, A. D., Hadly, E. A., Bascompte, J., Berlow, E. L., Brown, J. H., Fortelius, M., ... Smith, A. B.  
<sup>479</sup> (2012). Approaching a state shift in Earth’s biosphere. *Nature*, 486(7401), 52–58. doi:10.1038/nature11018
- <sup>480</sup> Bascompte, J., & Solé, R. V. (1996). Habitat fragmentation and extinction thresholds in spatially explicit  
<sup>481</sup> models. *Journal of Animal Ecology*, 65(4), 465–473. doi:10.2307/5781
- <sup>482</sup> Bazant, M. Z. (2000). Largest cluster in subcritical percolation. *Physical Review E*, 62(2), 1660–1669.  
<sup>483</sup> Retrieved from <http://link.aps.org/doi/10.1103/PhysRevE.62.1660>
- <sup>484</sup> Belward, A. S. (1996). *The IGBP-DIS Global 1 Km Land Cover Data Set “DISCover”: Proposal and*

- 485 *Implementation Plans : Report of the Land Recover Working Group of IGBP-DIS* (p. 61). IGBP-DIS Office.
- 486 Retrieved from <https://books.google.com.ar/books?id=qixsNAAACAAJ>
- 487 Benedetti-Cecchi, L., Tamburello, L., Maggi, E., & Bulleri, F. (2015). Experimental Perturbations Mod-
- 488 ify the Performance of Early Warning Indicators of Regime Shift. *Current Biology*, 25(14), 1867–1872.
- 489 doi:10.1016/j.cub.2015.05.035
- 490 Bestelmeyer, B. T., Duniway, M. C., James, D. K., Burkett, L. M., & Havstad, K. M. (2013). A test of
- 491 critical thresholds and their indicators in a desertification-prone ecosystem: more resilience than we thought.
- 492 *Ecology Letters*, 16, 339–345. doi:10.1111/ele.12045
- 493 Bestelmeyer, B. T., Ellison, A. M., Fraser, W. R., Gorman, K. B., Holbrook, S. J., Laney, C. M., ... Sharma,
- 494 S. (2011). Analysis of abrupt transitions in ecological systems. *Ecosphere*, 2(12), 129. doi:10.1890/ES11-
- 495 00216.1
- 496 Boettiger, C., & Hastings, A. (2012). Quantifying limits to detection of early warning for critical transitions.
- 497 *Journal of the Royal Society Interface*, 9(75), 2527–2539. doi:10.1098/rsif.2012.0125
- 498 Bonan, G. B. (2008). Forests and Climate Change: forcings, Feedbacks, and the Climate Benefits of Forests.
- 499 *Science*, 320(5882), 1444–1449. doi:10.1126/science.1155121
- 500 Botet, R., & Ploszajczak, M. (2004). Correlations in Finite Systems and Their Universal Scaling Properties.
- 501 In K. Morawetz (Ed.), *Nonequilibrium physics at short time scales: Formation of correlations* (pp. 445–466).
- 502 Berlin Heidelberg: Springer-Verlag.
- 503 Brook, B. W., Ellis, E. C., Perring, M. P., Mackay, A. W., & Blomqvist, L. (2013). Does the terrestrial
- 504 biosphere have planetary tipping points? *Trends in Ecology & Evolution*. doi:10.1016/j.tree.2013.01.016
- 505 Burnham, K., & Anderson, D. R. (2002). *Model selection and multi-model inference: A practical information-*
- 506 *theoretic approach* (2nd. ed., p. 512). New York: Springer-Verlag.
- 507 Canfield, D. E., Glazer, A. N., & Falkowski, P. G. (2010). The Evolution and Future of Earth's Nitrogen
- 508 Cycle. *Science*, 330(6001), 192–196. doi:10.1126/science.1186120
- 509 Carpenter, S. R., Cole, J. J., Pace, M. L., Batt, R., Brock, W. A., Cline, T., ... Weidel, B. (2011).
- 510 Early Warnings of Regime Shifts: A Whole-Ecosystem Experiment. *Science*, 332(6033), 1079–1082.
- 511 doi:10.1126/science.1203672
- 512 Clauset, A., Shalizi, C., & Newman, M. (2009). Power-Law Distributions in Empirical Data. *SIAM Review*,

- 513 51(4), 661–703. doi:10.1137/070710111
- 514 Corrado, R., Cherubini, A. M., & Pennetta, C. (2014). Early warning signals of desertification transitions  
515 in semiarid ecosystems. *Physical Review E - Statistical, Nonlinear, and Soft Matter Physics*, 90(6), 62705.  
516 doi:10.1103/PhysRevE.90.062705
- 517 Crawley, M. J. (2012). *The R Book* (2nd. ed., p. 1076). Hoboken, NJ, USA: Wiley.
- 518 Crowther, T. W., Glick, H. B., Covey, K. R., Bettigole, C., Maynard, D. S., Thomas, S. M., ... Bradford, M.  
519 A. (2015). Mapping tree density at a global scale. *Nature*, 525(7568), 201–205. doi:10.1038/nature14967
- 520 Dai, L., Vorselen, D., Korolev, K. S., & Gore, J. (2012). Generic Indicators for Loss of Resilience Before a  
521 Tipping Point Leading to Population Collapse. *Science*, 336(6085), 1175–1177. doi:10.1126/science.1219805
- 522 DiMiceli, C., Carroll, M., Sohlberg, R., Huang, C., Hansen, M., & Townshend, J. (2015). Annual Global Au-  
523 tomated MODIS Vegetation Continuous Fields (MOD44B) at 250 m Spatial Resolution for Data Years Begin-  
524 ning Day 65, 2000 - 2014, Collection 051 Percent Tree Cover, University of Maryland, College Park, MD, USA.  
525 Retrieved from [https://lpdaac.usgs.gov/dataset{\\\_}discovery/modis/modis{\\\_}products{\\\_}table/mod44b](https://lpdaac.usgs.gov/dataset{\_}discovery/modis/modis{\_}products{\_}table/mod44b)
- 526 Drake, J. M., & Griffen, B. D. (2010). Early warning signals of extinction in deteriorating environments.  
527 *Nature*, 467(7314), 456–459. doi:10.1038/nature09389
- 528 Efron, B., & Tibshirani, R. J. (1994). *An Introduction to the Bootstrap* (p. 456). New York: Taylor &  
529 Francis. Retrieved from <https://books.google.es/books?id=gLlpIUXRntoC>
- 530 Filotas, E., Parrott, L., Burton, P. J., Chazdon, R. L., Coates, K. D., Coll, L., ... Messier, C. (2014). Viewing  
531 forests through the lens of complex systems science. *Ecosphere*, 5(January), 1–23. doi:10.1890/ES13-00182.1
- 532 Foley, J. A., Ramankutty, N., Brauman, K. A., Cassidy, E. S., Gerber, J. S., Johnston, M., ... Zaks, D. P. M.  
533 (2011). Solutions for a cultivated planet. *Nature*, 478(7369), 337–342. doi:10.1038/nature10452
- 534 Folke, C., Jansson, Å., Rockström, J., Olsson, P., Carpenter, S. R., Iii, F. S. C., ... Westley, F. (2011).  
535 Reconnecting to the Biosphere. *AMBIO*, 40(7), 719–738. doi:10.1007/s13280-011-0184-y
- 536 Fung, T., O'Dwyer, J. P., Rahman, K. A., Fletcher, C. D., & Chisholm, R. A. (2016). Reproducing static  
537 and dynamic biodiversity patterns in tropical forests: the critical role of environmental variance. *Ecology*,  
538 97(5), 1207–1217. doi:10.1890/15-0984.1
- 539 Gardner, R. H., & Urban, D. L. (2007). Neutral models for testing landscape hypotheses. *Landscape Ecology*,  
540 22(1), 15–29. doi:10.1007/s10980-006-9011-4
- 541 Gastner, M. T., Oborny, B., Zimmermann, D. K., & Pruessner, G. (2009). Transition from Connected

- 542 to Fragmented Vegetation across an Environmental Gradient: Scaling Laws in Ecotone Geometry. *The*  
543 *American Naturalist*, 174(1), E23–E39. doi:10.1086/599292
- 544 Gilman, S. E., Urban, M. C., Tewksbury, J., Gilchrist, G. W., & Holt, R. D. (2010). A framework  
545 for community interactions under climate change. *Trends in Ecology & Evolution*, 25(6), 325–331.  
546 doi:10.1016/j.tree.2010.03.002
- 547 Goldstein, M. L., Morris, S. A., & Yen, G. G. (2004). Problems with fitting to the power-law distri-  
548 bution. *The European Physical Journal B - Condensed Matter and Complex Systems*, 41(2), 255–258.  
549 doi:10.1140/epjb/e2004-00316-5
- 550 Haddad, N. M., Brudvig, L. a., Clobert, J., Davies, K. F., Gonzalez, A., Holt, R. D., ... Townshend, J. R.  
551 (2015). Habitat fragmentation and its lasting impact on Earth's ecosystems. *Science Advances*, 1(2), 1–9.  
552 doi:10.1126/sciadv.1500052
- 553 Hansen, M. C., Potapov, P. V., Moore, R., Hancher, M., Turubanova, S. A., Tyukavina, A., ... Townshend,  
554 J. R. G. (2013). High-Resolution Global Maps of 21st-Century Forest Cover Change. *Science*, 342(6160),  
555 850–853. doi:10.1126/science.1244693
- 556 Hansen, M., Potapov, P., Margono, B., Stehman, S., Turubanova, S., & Tyukavina, A. (2014). Response  
557 to Comment on “High-resolution global maps of 21st-century forest cover change”. *Science*, 344(6187), 981.  
558 doi:10.1126/science.1248817
- 559 Hantson, S., Pueyo, S., & Chuvieco, E. (2015). Global fire size distribution is driven by human impact and  
560 climate. *Global Ecology and Biogeography*, 24(1), 77–86. doi:10.1111/geb.12246
- 561 Harris, T. E. (1974). Contact interactions on a lattice. *The Annals of Probability*, 2, 969–988.
- 562 Hartigan, J. A., & Hartigan, P. M. (1985). The Dip Test of Unimodality. *The Annals of Statistics*, 13(1),  
563 70–84. Retrieved from <http://www.jstor.org/stable/2241144>
- 564 Hastings, A., & Wysham, D. B. (2010). Regime shifts in ecological systems can occur with no warning.  
565 *Ecology Letters*, 13(4), 464–472. doi:10.1111/j.1461-0248.2010.01439.x
- 566 He, F., & Hubbell, S. (2003). Percolation Theory for the Distribution and Abundance of Species. *Physical*  
567 *Review Letters*, 91(19), 198103. doi:10.1103/PhysRevLett.91.198103
- 568 Hinrichsen, H. (2000). Non-equilibrium critical phenomena and phase transitions into absorbing states.  
569 *Advances in Physics*, 49(7), 815–958. doi:10.1080/00018730050198152
- 570 Hirota, M., Holmgren, M., Nes, E. H. V., & Scheffer, M. (2011). Global Resilience of Tropical Forest and

- 571 Savanna to Critical Transitions. *Science*, 334(6053), 232–235. doi:10.1126/science.1210657
- 572 Irvine, M. A., Bull, J. C., & Keeling, M. J. (2016). Aggregation dynamics explain vegetation patch-size  
573 distributions. *Theoretical Population Biology*, 108, 70–74. doi:10.1016/j.tpb.2015.12.001
- 574 Keitt, T. H., Urban, D. L., & Milne, B. T. (1997). Detecting critical scales in fragmented landscapes.  
575 *Conservation Ecology*, 1(1), 4. Retrieved from <http://www.ecologyandsociety.org/vol1/iss1/art4/>
- 576 Kéfi, S., Guttal, V., Brock, W. A., Carpenter, S. R., Ellison, A. M., Livina, V. N., ... Dakos, V. (2014).  
577 Early Warning Signals of Ecological Transitions: Methods for Spatial Patterns. *PLoS ONE*, 9(3), e92097.  
578 doi:10.1371/journal.pone.0092097
- 579 Kéfi, S., Rietkerk, M., Alados, C. L., Pueyo, Y., Papanastasis, V. P., ElAich, A., & Ruiter, P. C. de.  
580 (2007). Spatial vegetation patterns and imminent desertification in Mediterranean arid ecosystems. *Nature*,  
581 449(7159), 213–217. doi:10.1038/nature06111
- 582 Kitzberger, T., Aráoz, E., Gowda, J. H., Mermoz, M., & Morales, J. M. (2012). Decreases in Fire Spread  
583 Probability with Forest Age Promotes Alternative Community States, Reduced Resilience to Climate Vari-  
584 ability and Large Fire Regime Shifts. *Ecosystems*, 15(1), 97–112. doi:10.1007/s10021-011-9494-y
- 585 Koenker, R. (2016). quantreg: Quantile Regression. Retrieved from <http://cran.r-project.org/package=quantreg>
- 586 Lasco, R. D., Pulhin, F. B., Cruz, R. V. O., Pulhin, J. M., Roy, S. S. N., & Sanchez, P. A. J. (2008). Forest  
587 responses to changing rainfall in the Philippines. In N. Leary, C. Conde, & J. Kulkarni (Eds.), *Climate  
588 change and vulnerability* (pp. 49–66). London: Earthscan. Retrieved from <http://gen.lib.rus.ec/book/index.php?md5=AD313B13E05C9D61A9EC1EE2E73A91FB>
- 589
- 590 Leibold, M. A., & Norberg, J. (2004). Biodiversity in metacommunities: Plankton as complex adaptive  
591 systems? *Limnology and Oceanography*, 49(4, part 2), 1278–1289. doi:10.4319/lo.2004.49.4\_part\_2.1278
- 592
- 593 Lenton, T. M., & Williams, H. T. P. (2013). On the origin of planetary-scale tipping points. *Trends in  
594 Ecology & Evolution*, 28(7), 380–382. doi:10.1016/j.tree.2013.06.001
- 595 Limpert, E., Stahel, W. A., & Abbt, M. (2001). Log-normal Distributions across the Sciences: Keys and  
596 CluesOn the charms of statistics, and how mechanical models resembling gambling machines offer a link to  
597 a handy way to characterize log-normal distributions, which can provide deeper insight into var. *BioScience*,  
598 51(5), 341–352. Retrieved from [http://dx.doi.org/10.1641/0006-3568\(2001\)051\[0341:LNDATS\]2.0.CO](http://dx.doi.org/10.1641/0006-3568(2001)051[0341:LNDATS]2.0.CO)
- 599 Loehle, C., Li, B.-L., & Sundell, R. C. (1996). Forest spread and phase transitions at forest-prairie ecotones

- 600 in Kansas, U.S.A. *Landscape Ecology*, 11(4), 225–235.
- 601 Malhi, Y., Gardner, T. A., Goldsmith, G. R., Silman, M. R., & Zelazowski, P. (2014). Tropical Forests in  
602 the Anthropocene. *Annual Review of Environment and Resources*, 39(1), 125–159. doi:10.1146/annurev-  
603 environ-030713-155141
- 604 Manor, A., & Shnerb, N. M. (2008). Origin of pareto-like spatial distributions in ecosystems. *Physical*  
605 *Review Letters*, 101(26), 268104. doi:10.1103/PhysRevLett.101.268104
- 606 Martensen, A. C., Ribeiro, M. C., Banks-Leite, C., Prado, P. I., & Metzger, J. P. (2012). Associations  
607 of Forest Cover, Fragment Area, and Connectivity with Neotropical Understory Bird Species Richness and  
608 Abundance. *Conservation Biology*, 26(6), 1100–1111. doi:10.1111/j.1523-1739.2012.01940.x
- 609 McKenzie, D., & Kennedy, M. C. (2012). Power laws reveal phase transitions in landscape con-  
610 trols of fire regimes. *Nat Commun*, 3, 726. Retrieved from <http://dx.doi.org/10.1038/ncomms1731>  
611 [http://www.nature.com/ncomms/journal/v3/n3/suppinfo/ncomms1731{\\\_\\\_}S1.html](http://www.nature.com/ncomms/journal/v3/n3/suppinfo/ncomms1731{\_\_}S1.html)
- 612 Mitchell, M. G. E., Suarez-Castro, A. F., Martinez-Harms, M., Maron, M., McAlpine, C., Gaston, K. J., ...  
613 Rhodes, J. R. (2015). Reframing landscape fragmentation's effects on ecosystem services. *Trends in Ecology*  
614 & Evolution, 30(4), 190–198. doi:10.1016/j.tree.2015.01.011
- 615 Naito, A. T., & Cairns, D. M. (2015). Patterns of shrub expansion in Alaskan arctic river corridors suggest  
616 phase transition. *Ecology and Evolution*, 5(1), 87–101. doi:10.1002/ece3.1341
- 617 Newman, M. E. J. (2005). Power laws, Pareto distributions and Zipf's law. *Contemporary Physics*, 46(5),  
618 323–351. doi:10.1080/00107510500052444
- 619 Oborny, B., Meszéna, G., & Szabó, G. (2005). Dynamics of Populations on the Verge of Extinction. *Oikos*,  
620 109(2), 291–296. Retrieved from <http://www.jstor.org/stable/3548746>
- 621 Oborny, B., Szabó, G., & Meszéna, G. (2007). Survival of species in patchy landscapes: percolation in  
622 space and time. In *Scaling biodiversity* (pp. 409–440). Cambridge University Press. Retrieved from <http://dx.doi.org/10.1017/CBO9780511814938.022>
- 624 Ochoa-Quintero, J. M., Gardner, T. A., Rosa, I., de Barros Ferraz, S. F., & Sutherland, W. J. (2015).  
625 Thresholds of species loss in Amazonian deforestation frontier landscapes. *Conservation Biology*, 29(2),  
626 440–451. doi:10.1111/cobi.12446
- 627 Ódor, G. (2004). Universality classes in nonequilibrium lattice systems. *Reviews of Modern Physics*, 76(3)

- 628 I), 663–724. doi:10.1103/RevModPhys.76.663
- 629 Pardini, R., Bueno, A. de A., Gardner, T. A., Prado, P. I., & Metzger, J. P. (2010). Beyond the Fragmen-  
630 tation Threshold Hypothesis: Regime Shifts in Biodiversity Across Fragmented Landscapes. *PLoS ONE*,  
631 5(10), e13666. doi:10.1371/journal.pone.0013666
- 632 Potapov, P., Yaroshenko, A., Turubanova, S., Dubinin, M., Laestadius, L., Thies, C., ... Zhuravleva, I. (2008).  
633 Mapping the world's intact forest landscapes by remote sensing. *Ecology and Society*, 13(2).
- 634 Pueyo, S., de Alencastro Graça, P. M. L., Barbosa, R. I., Cots, R., Cardona, E., & Fearnside, P. M. (2010).  
635 Testing for criticality in ecosystem dynamics: the case of Amazonian rainforest and savanna fire. *Ecology  
Letters*, 13(7), 793–802. doi:10.1111/j.1461-0248.2010.01497.x
- 637 R Core Team. (2015). R: A Language and Environment for Statistical Computing. Vienna, Austria: R  
638 Foundation for Statistical Computing. Retrieved from <http://www.r-project.org/>
- 639 Reyer, C. P. O., Rammig, A., Brouwers, N., & Langerwisch, F. (2015). Forest resilience, tipping points and  
640 global change processes. *Journal of Ecology*, 103(1), 1–4. doi:10.1111/1365-2745.12342
- 641 Rockstrom, J., Steffen, W., Noone, K., Persson, A., Chapin, F. S., Lambin, E. F., ... Foley, J. A. (2009). A  
642 safe operating space for humanity. *Nature*, 461(7263), 472–475. Retrieved from [http://dx.doi.org/10.1038/461472a](http://dx.doi.org/10.1038/<br/>643 461472a)
- 644 Rooij, M. M. J. W. van, Nash, B., Rajaraman, S., & Holden, J. G. (2013). A Fractal Approach to Dynamic  
645 Inference and Distribution Analysis. *Frontiers in Physiology*, 4(1). doi:10.3389/fphys.2013.00001
- 646 Saravia, L. A., & Momo, F. R. (2017). Biodiversity collapse and early warning indicators in  
647 a spatial phase transition between neutral and niche communities. *PeerJ PrePrints*, 5, e1589v4.  
648 doi:10.7287/peerj.preprints.1589v3
- 649 Scanlon, T. M., Caylor, K. K., Levin, S. A., & Rodriguez-iturbe, I. (2007). Positive feedbacks promote  
650 power-law clustering of Kalahari vegetation. *Nature*, 449(September), 209–212. doi:10.1038/nature06060
- 651 Scheffer, M., Bascompte, J., Brock, W. A., Brovkin, V., Carpenter, S. R., Dakos, V., ... Sugihara, G. (2009).  
652 Early-warning signals for critical transitions. *Nature*, 461(7260), 53–59. doi:10.1038/nature08227
- 653 Scheffer, M., Walker, B., Carpenter, S., Foley, J. a, Folke, C., & Walker, B. (2001). Catastrophic shifts in  
654 ecosystems. *Nature*, 413(6856), 591–596. doi:10.1038/35098000
- 655 Seidler, T. G., & Plotkin, J. B. (2006). Seed Dispersal and Spatial Pattern in Tropical Trees. *PLoS Biology*,

- 656 4(11), e344. doi:10.1371/journal.pbio.0040344
- 657 Sexton, J. O., Noojipady, P., Song, X.-P., Feng, M., Song, D.-X., Kim, D.-H., ... Townshend, J. R.  
658 (2015). Conservation policy and the measurement of forests. *Nature Climate Change*, 6(2), 192–196.  
659 doi:10.1038/nclimate2816
- 660 Sexton, J. O., Song, X.-P., Feng, M., Noojipady, P., Anand, A., Huang, C., ... Townshend, J. R. (2013).  
661 Global, 30-m resolution continuous fields of tree cover: Landsat-based rescaling of MODIS vegetation con-  
662 tinuous fields with lidar-based estimates of error. *International Journal of Digital Earth*, 6(5), 427–448.  
663 doi:10.1080/17538947.2013.786146
- 664 Sole, R. V., Alonso, D., & Mckane, A. (2002). Self-organized instability in complex ecosystems. *Philoso-  
665 sophical Transactions of the Royal Society of London. Series B, Biological Sciences*, 357(May), 667–681.  
666 doi:10.1098/rstb.2001.0992
- 667 Solé, R. V. (2011). *Phase Transitions* (p. 223). Princeton University Press. Retrieved from <https://books.google.com.ar/books?id=8RcLuv-Ll2kC>
- 669 Solé, R. V., & Bascompte, J. (2006). *Self-organization in complex ecosystems* (p. 373). New Jersey, USA.:  
670 Princeton University Press. Retrieved from <http://books.google.com.ar/books?id=v4gpGH6Gv68C>
- 671 Solé, R. V., Alonso, D., & Saldaña, J. (2004). Habitat fragmentation and biodiversity collapse in neutral  
672 communities. *Ecological Complexity*, 1(1), 65–75. doi:10.1016/j.ecocom.2003.12.003
- 673 Solé, R. V., Bartumeus, F., & Gamarra, J. G. P. (2005). Gap percolation in rainforests. *Oikos*, 110(1),  
674 177–185. doi:10.1111/j.0030-1299.2005.13843.x
- 675 Stauffer, D., & Aharony, A. (1994). *Introduction To Percolation Theory* (p. 179). London: Taylor & Francis.
- 676 Staver, A. C., Archibald, S., & Levin, S. A. (2011). The Global Extent and Determinants of Savanna and  
677 Forest as Alternative Biome States. *Science*, 334(6053), 230–232. doi:10.1126/science.1210465
- 678 Vasilakopoulos, P., & Marshall, C. T. (2015). Resilience and tipping points of an exploited fish population  
679 over six decades. *Global Change Biology*, 21(5), 1834–1847. doi:10.1111/gcb.12845
- 680 Verbesselt, J., Umlauf, N., Hirota, M., Holmgren, M., Van Nes, E. H., Herold, M., ... Scheffer, M. (2016). Re-  
681 motely sensed resilience of tropical forests. *Nature Climate Change*, 1(September). doi:10.1038/nclimate3108
- 682 Villa Martín, P., Bonachela, J. A., & Muñoz, M. A. (2014). Quenched disorder forbids discontinuous  
683 transitions in nonequilibrium low-dimensional systems. *Physical Review E*, 89(1), 12145. Retrieved from

- 684 <https://link.aps.org/doi/10.1103/PhysRevE.89.012145>
- 685 Villa Martín, P., Bonachela, J. A., Levin, S. A., & Muñoz, M. A. (2015). Eluding catastrophic shifts.
- 686 *Proceedings of the National Academy of Sciences*, 112(15), E1828–E1836. doi:10.1073/pnas.1414708112
- 687 Viña, A., McConnell, W. J., Yang, H., Xu, Z., & Liu, J. (2016). Effects of conservation policy on China's  
688 forest recovery. *Science Advances*, 2(3), e1500965. Retrieved from <http://advances.sciencemag.org/content/2/3/e1500965.abstract>
- 689
- 690 Vuong, Q. H. (1989). Likelihood Ratio Tests for Model Selection and Non-Nested Hypotheses. *Econometrica*,  
691 57(2), 307–333. doi:10.2307/1912557
- 692 Weerman, E. J., Van Belzen, J., Rietkerk, M., Temmerman, S., Kéfi, S., Herman, P. M. J., & Koppell, J. V.  
693 de. (2012). Changes in diatom patch-size distribution and degradation in a spatially self-organized intertidal  
694 mudflat ecosystem. *Ecology*, 93(3), 608–618. doi:10.1890/11-0625.1
- 695 Weissmann, H., & Shnerb, N. M. (2016). Predicting catastrophic shifts. *Journal of Theoretical Biology*, 397,  
696 128–134. doi:10.1016/j.jtbi.2016.02.033
- 697 Wuyts, B., Champneys, A. R., & House, J. I. (2017). Amazonian forest-savanna bistability and human  
698 impact. *Nature Communications*, 8(May), 15519. doi:10.1038/ncomms15519
- 699 Xu, C., Hantson, S., Holmgren, M., Nes, E. H. van, Staal, A., & Scheffer, M. (2016). Remotely sensed  
700 canopy height reveals three pantropical ecosystem states. *Ecology*, 97(9), 2518–2521. doi:10.1002/ecy.1470
- 701 Zhang, J. Y., Wang, Y., Zhao, X., Xie, G., & Zhang, T. (2005). Grassland recovery by protection from  
702 grazing in a semi-arid sandy region of northern China. *New Zealand Journal of Agricultural Research*, 48(2),  
703 277–284. doi:10.1080/00288233.2005.9513657
- 704 Zinck, R. D., & Grimm, V. (2009). Unifying wildfire models from ecology and statistical physics. *The  
705 American Naturalist*, 174(5), E170–85. doi:10.1086/605959